Inactivation of marine heterotrophic bacteria in ballast water by an Electrochemical Advanced Oxidation Process

Javier Moreno-Andrés[1], Noemi Ambauen[2], Olav Vadstein[3], Cynthia Hallé[2], Asunción Acevedo-Merino[1], Enrique Nebot[1] and Thomas Meyn[2]

[1]Department of Environmental Technologies. INMAR-Marine Research Institute. University of Cádiz. Campus Universitario Puerto Real, 11510 - Puerto Real. Cádiz. Spain.

[2]Department of Civil and Environmental Engineering, NTNU Norwegian University of Science and Technology, N-7491 Trondheim, Norway

[3] Department of Biotechnology and Food Science, NTNU Norwegian University of Science and Technology, N-7491 Trondheim, Norway.

*Corresponding Author. Javier Moreno-Andrés.

E-mail address: javier.moreno@uca.es (J. Moreno)

Abstract

Seawater treatment is increasingly required due to industrial activities that use substantial volumes of seawater in their processes. The shipping industry and the associated management of a ship´s ballast water are currently considered a global challenge for the seas. Related to that, the suitability of an Electrochemical Advanced Oxidation Process (EAOP) with Boron Doped Diamond (BDD) electrodes has been assessed on a laboratory scale for the disinfection of seawater. This technology can produce both reactive oxygen species and chlorine species (especially in seawater) that are responsible for inactivation. The EAOP was applied in a continuous-flow regime with real seawater. Natural marine heterotrophic bacteria (MHB) were used as an indicator of disinfection efficiency. A biphasic inactivation kinetic model was fitted on experimental points, achieving 4-Log reductions at 0.019 $Ah \cdot L^{-1}$. By assessing regrowth after treatment, results suggest that higher bacterial damages result from the EAOP

when it is compared to chlorination. Furthermore, several issues lacking fundamental understanding were investigated such as recolonization capacity or bacterial community dynamics. It was concluded that, despite disinfection processes being effective, there is not only a possibility for regrowth after treatment but also a change on bacterial population diversity produced by the treatment. Finally, energy consumption was estimated and indicated that 0.264 $kWh \cdot m^{-3}$ are needed for 4.8-Log reductions of MHB; otherwise, with 0.035 $kWh \cdot m^{-3}$, less disinfection efficiency can be obtained (2.2-Log red). However, with a residual oxidant in the solution, total inactivation can be achieved in three days.

Key Words:

Ballast water treatment, marine bacteria, chlorine active species, ROS, recolonization, bacterial diversity

1. Introduction

The treatment of seawater has experienced increased interest related to industrial activities that utilize substantial volumes of seawater in processes such as aquaculture or shipping. It implies associated risks due to the control of pathogens or undesired biofouling that must be prevented (De Schryver and Vadstein, 2014; Oh et al., 2010; Tanaka et al., 2013). Maritime transport deserves special attention; in 2015, world seaborne trade volumes were estimated to have exceeded ten billion tons which means that 80% of international trade is conducted by sea (UNCTAD, 2016). Related to that, an emerging challenge associated with a ship´s ballast water has been related to the introduction of aquatic invasive species. Currently, it is considered as the fourth greatest threat to the world´s oceans (GEF-UNDP-IMO, 2017; UNCTAD, 2016). Thus, the "International Convention on the Management of Ships' Ballast Water and Sediments" (BWMC) was adopted in 2004 and has recently been entered into force (September-2017) (IMO, 2004). Among several specific aspects, the BWMC requires that ballast water must be treated in accordance with discharge limits established in Rule D2. It distinguished five organism groups with three being indicator microbes (*E. coli*, *Enterococci* and *V. cholerae*).

These microbiological standards are proposed in order to avoid the introduction of undesired aquatic microorganisms. Bacterial indicators are otherwise primarily centered on human health concerns and do not consider the risks associated with other coastal activities. It specifically implies to additional aquatic bacteria or viruses which could cause epidemics/epizootics or other ecosystem consequences. Besides, some authors indicate that specific indicator microbes standards that are established in the BWMC were identified at low concentrations in ballast water samples (Cohen and Dobbs, 2015; Lymperopoulou and Dobbs, 2017). In parallel, other studies showed the high diversity of marine bacteria in ballast tanks (Brinkmeyer, 2016; Lymperopoulou and Dobbs,

65 2017) which suggests that other bacterial indicators, such as Marine Heterotrophic
66 Bacteria (MHB), should be incorporated into the regulations.

67 Nevertheless, the entry into force of the BWMC requires the implementation of
68 seawater disinfection systems. In this aspect, several studies have been conducted to
69 propose a number of options for treating ballast water that take into account
70 environmental, technical, and economic criteria (LLoyd`s Register Maritime, 2017;
71 Tsolaki and Diamadopoulos, 2010). A number of challenges in this regard are the ability
72 of working with high ballasting and discharge flow-rates as well as ensuring their
73 effectiveness in seawater that is characterized by high salinity and high microbiological
74 activity. On the other hand, even though a wide range of studies focused on treatment
75 efficiency, there is limited literature focusing on side effects caused by disinfection. It
76 implies the regrowth potential in ballast tanks (Grob and Pollet, 2016) or the hazards
77 associated with the alteration on dynamics of bacterial communities after disinfection,
78 which seems to be an emerging challenge (Hess-Erga et al., 2010).

79 Chemical disinfection such as chlorination or using several biocides is problematic if it
80 needs to be used onboard due to the transport and storage of active substances. Besides,
81 depending on the water matrix composition, the generation of hazardous by-products
82 could be an issue of major concern (Werschkun et al., 2012). UV-disinfection is another
83 well-established method for this purpose, however, it has a disadvantage which is the
84 repair mechanisms of microorganisms and consequential regrowth, especially in these
85 types of waters (Grob and Pollet, 2016; Moreno-Andrés et al., 2018; Romero-Martínez
86 et al., 2016). Advanced Oxidation Processes (AOPs) are considered as an alternative
87 option for water treatment. They have mainly been focused on the disinfection of
88 drinking water and the removal of hardly biodegradable organic pollutants in
89 wastewaters (Chaplin, 2014; Comninellis and Chen, 2010). However, AOPs in seawater

have been poorly developed for these purposes (Aguilar et al., 2017; Moreno-Andrés et al., 2017; Rubio et al., 2013; Särkkä et al., 2015).

An attractive alternative is the *in-situ* generation of oxidant species as in the case of Electrochemical Advanced Oxidation Processes (EAOPs). They have gained significance through the years by providing high efficiency in drinking water and in both industrial and domestic wastewater treatment systems (Chaplin, 2014; Garcia-Segura et al., 2017; Moreira et al., 2017; Särkkä et al., 2015). Even in ballast water or aquaculture applications high inactivation rates have been reached; e.g., with low energy requirements for *E. coli* (Nanayakkara et al., 2012), as well as in different types of marine organisms (Cha et al., 2015; Oh et al., 2010; Tanaka et al., 2013; Tsolaki et al., 2010). However, these studies used active electrodes with low oxygen evolution overpotential. This only permits the application of low currents before oxygen evolution begins and, consequently, competitive reactions occur that result in the major consumption of radical species and thus lower efficiency (Comninellis and Chen, 2010; Jeong et al., 2009). Additionally, active electrodes also favor the direct oxidation of chloride ions at the electrode surface to form chlorine (Garcia-Segura et al., 2017; Jeong et al., 2006; Panizza and Cerisola, 2009).

With the aim to assess powerful oxidizing treatments that could achieve high disinfection efficiency together with the avoidance of bacterial regrowth, the use of non-active electrodes can be a valid candidate for seawater treatment (Vacca et al., 2013). With non-active electrodes, higher efficiencies in the electro-generation of Reactive Oxygen Species (ROS) can be achieved due to the high overpotential for oxygen evolution (Eq. (1-4)) (Garcia-Segura et al., 2017; Panizza and Cerisola, 2009; Vacca et al., 2013). Thus, a combination of ROS oxidation and active chlorine generation could take part in disinfection mechanisms (Jeong et al., 2006). Therefore, among the major advantages of the non-active materials, such as the high mechanical strength and

chemical inertness, •OH are physisorbed on the anode surface and higher inactivation rates may be reached; i.e., non-active anode promotes •OH diffusion to the bulk and reduces competing reactions (Comninellis and Chen, 2010; Jeong et al., 2009; Moreira et al., 2017).

$$H_2O \rightarrow \bullet OH + H^+ + e^- \quad \text{Eq. (1)}$$

$$\bullet OH \rightarrow \bullet O + H^+ + e^- \quad \text{Eq. (2)}$$

$$\bullet O + O_2 \rightarrow O_3 \quad \text{Eq. (3)}$$

$$\bullet OH + \bullet OH \rightarrow H_2O_2 \quad \text{Eq. (4)}$$

A clear example is the use of Boron Doped Diamond (BDD) as anode material (Chaplin, 2014). It has previously been studied for disinfection of seawater, e.g., Lacasa et al. (2013) evaluated disinfection efficiency on *Artemia salina* and *E. coli*; Petrucci et al. (2013) obtained strong inactivation effects for marine dinoflagellates and marine bacterium *P. aeruginosa*. However, those studies work either at batch mode (implies an electrolysis time in the order of minutes) or at very low flow-rates, an aspect that is not feasible in the case of ballast water treatments (BWTs) that require high ballasting/deballasting flow-rates.

In this context, the EAOP with BDD electrodes was evaluated, and their operation was optimized for disinfection of seawater by assessing both inactivation kinetics and regrowth capability following treatment. The application of this process in a continuous-flow regime with real seawater and natural marine heterotrophic bacteria (MHB) as an indicator of disinfection efficiency is the main novelty aspect. Furthermore, an approach of bacterial community dynamics after treatment has been performed; this is a factor that is extremely challenging in the case of ballast water discharges. Finally, a comparison of the disinfection efficiency between the EAOP and NaOCl (added as a chemical) has been performed to investigate the bacterial survival on both processes.

2. Material and Methods

2.1 Water sampling

Seawater (SW) samples were collected from Trondheimfjord (Trondheim, Norway). SW was pumped from 70 m deep at SeaLab (NTNU Centre of Fisheries and Aquaculture) and, following the sand-filter step, they were collected in 25 L tanks and used as a water matrix for experimental assays.

Physicochemical characterization of the water used in the experiments was performed (Table 1) including conductivity, pH, temperature (HQ430D-Hach), and turbidity (2100AN-Hach, laboratory turbidimeter). A Total Organic Carbon (TOC) analysis was conducted using an Apollo 9000 TOC Analyzer. Alkalinity was determined by a titration using hydrochloric acid (HCl) 0.02M (AVS Titrinorm, VRW). Different ions were analyzed by ion chromatography (881- Compact IC Pro; 882-Compact IC Plus, Metrohm) with detection by conductivity.

2.2 Electrolytic cell and Experimental set-up

Experiments were performed in a DiaClean® Lab Unit (WaterDiam) with Electrolytic cell DiaClean® 106.101 which consists of two monopolar circular Si/BDD electrodes (Boron Doped Diamond on Silicon substrate); their active surface is 70 cm^2 with an electrode gap of 1 mm. The electrical power was supplied by a DC power supply (DiaClean®–PS 1000) polarity reversal function with tunable frequencies. The range of possible applied current was between 0.6 up to 19 A.

2.2.1 Inactivation assays

Experiments were conducted in a single pass with seawater pumped in once from the storage tank (20 L) through the electrolytic cell at different flow-rates (200-1000 $L \cdot h^{-1}$) and various current values (0.7-7.3A), which corresponds to current density ranging between 9.72-101.38 $mA \cdot cm^{-2}$ and implying different electrical charges applied (Q)

(Fig A1, Supp. material). Theoretical Retention Time (TRT) on electrolytic cell ranged from 0.13 - 0.03 s.

Before each battery of assays, the Lab Unit was cleaned and disinfected with sodium hypochlorite and then rinsed with sterile water. During this cleaning procedure, polarity was automatically inverted every ten minutes to avoid operational problems such as the formation of coatings or any material on the electrode surfaces from previous runs.

Each sample was collected in a sterile 250 mL flask at the outlet once the flow-rate was stabilized. First, a similar volume to the total system volume was wasted, and the sample was subsequently collected in an ascending flow-rate (to avoid possible microbiological contamination). At the beginning of the assay, a control sample was taken to determine the initial bacterial concentration. Additionally, a mechanical stress control was performed with the run at 0 $mA \cdot cm^{-2}$ (no changes with the control were detected). Samples in the same experimental series were taken during a time lapse of 20 minutes maximum and stored in a cool, dark place until microbiological analysis.

Each sample (different flow rate/current) was collected in two sterile flasks. One was collected with a quenching agent in order to determine survival bacterial and assure that the electro-generated Total Residual Oxidants (TRO) did not have bactericidal effects after treatment. The other was collected by keeping the TRO in a solution with the aim of assessing the residual effects after treatment.

2.2.2 Recolonization assays

Survival and recolonization of marine heterotrophic bacteria were investigated after the disinfection procedures by replicating a system of ballast water treatment in which water was stored in ballast tanks during a voyage. In this context, five samples were selected in varying degrees of inactivation produced by different values of the TRO that was generated (Unt., S1, S2, S3, S4) with Unt. being the untreated sample (initial

control). The experimental procedure was similar to the previous section: collecting samples in 250 ml flasks (previously sterilized by autoclave), collecting them twice, quenching the TRO, and keeping it in a solution. The five samples (Unt., S1, S2, S3, S4) were stored in the dark at 20 ºC. Each day, the bacterial concentration and TRO were measured according to Sections 2.3 and 2.4, respectively.

Each battery of assays was repeated in three independent moments. Statistical differences between each sample with controls were evaluated by analysis of variance (ANOVA) using Statgraphics® Centurion XVII (Version 17.0.16-Statpoints Technologies, Inc.).

2.3 Microbiological procedures

Natural Marine Heterotrophic Bacteria (MHB) was assessed as an indicator of disinfection efficiency. Following IMO recommendations (BWMC, G8-Guideline), a minimum concentration of 10^4 Colony-Forming Unit (CFU) per mL is needed for inactivation assays. To obtain that concentration and secure good statistics, yeast extract was added as a substrate for MHB. Four equal amounts were added at 0, 3, 6, and 12 hours (total of 2 $\mu g \cdot mL^{-1}$). All assays began 48 hours after water sampling.

Bacterial survival after treatment was assessed by colony counting: samples were plated in triplicate on petri dishes with Difco™ Marine Agar 2216 (detection limit, 2 $CFU \cdot mL^{-1}$). Petri plates were inverted and incubated at 20°C for five days. To assure valid counts on petri plates, ten-fold dilutions were performed, and the majority of agar plates used for quantification had 10-150 CFU. With three replicates per sample, we obtained a coefficient variation of ≤ 30%. After yeast extract additions, the initial concentration of MHB was approximately 10^6 $CFU \cdot mL^{-1}$ which gives a disinfection detection limit of -5.70 decimal log units, log (N/N_0). Sterile conditions were monitored with plating blank samples during the microbiological analytical procedure.

2.3.1 Estimates of bacterial diversity

A plate count method based on the time required to form macroscopically visible colonies (Tv, days) was used. Tv is linearly related to the maximum specific growth rate, therefore, divides the culturable MHB into categories based on their maximum growth rate. This is a simple methodology that requires no specialized equipment and is applicable for describing the community structure with special reference to r/K-theory (Salvesen and Vadstein, 2000).

The procedure followed the protocol of Salvesen and Vadstein, (2000). Briefly, samples from three independent experiments were spread in triplicate on agar and incubated at 20 ºC (each day during a period of eight days). An untreated sample was used as a model of natural seawater, i.e., freshly collected water samples. CFUs were counted regularly after plating to obtain differences in the frequency distribution of visible colonies as a function of time after plating. Colonies had to have a diameter >0.2 mm to be considered visible. Thus, colonies that belonged to bacterial groups with high growth rates would be visible on the first or second day after plating whereas those with slower growth rates would take longer to develop visible colonies. In this aspect, with the aim of obtaining a parameter with biological interpretation, the percentage of rapidly grown colonies was obtained, i.e., colonies that showed Tv=1 and 2 in respect to the total. This is directly related to the theory of r and K strategists because opportunistic bacteria (r-strategists) are distinct from non-opportunistic (K-strategists) according to their high maximum growth rate (De Schryver and Vadstein, 2014; Salvesen and Vadstein, 2000).

2.3.2 Microbiological data analysis

Modeling of inactivation kinetics was performed according to different types of microbial survival models (Geeraerd et al., 2005). The most suitable for this case was the biphasic model, according to Eq. (5) (Cerf, 1977).

241 $N=N_0\left[f \cdot e^{-k_1 Q} + (1-f)e^{-k_2 Q}\right]$ Eq. (5)

242 Parameters in the model are: electrical charge applied (Q, $Ah \cdot L^{-1}$); first and second
243 disinfection rate constants (k_1, k_2, $L \cdot Ah^{-1}$); and the fraction of the initial organisms that
244 follows a fast disinfection route (***f***, associated to k_1). The validity of this model was
245 evaluated by the coefficient of determination (R^2) and the Root Mean Square Error
246 (RMSE).

247 For regrowth analysis, the percentage of bacterial regrowth was calculated according to
248 Eq. (6) based on the concentration of viable bacteria ($CFU \cdot mL^{-1}$) before (N_0) and after
249 (N) disinfection treatment as well as in the regrowth sample (N_t) (Lindenauer and
250 Darby, 1994).

251 $\%\, repair = \frac{N_t - N}{N_0 - N} \cdot 100\%$ Eq. (6)

252 ***2.4 Chemicals and analytical methods***

253 In addition to the EAOP application, parallel assays were performed with sodium
254 hypochlorite (NaClO solution 10% w/v, Sigma-Aldrich) added as a chemical in order to
255 compare the effects of electro-generated TRO in bacterial inactivation. Sodium
256 thiosulfate pentahydrate ($Na_2S_2O_3 \cdot 5H_2O$, Sigma-Aldrich) was used for TRO quenching
257 at a ratio of 3 mol of $Na_2S_2O_3 \cdot 5H_2O$ for every mol of chlorine in the samples. It was
258 placed in sterile flasks before sampling in order to achieve instant TRO neutralization.

259 The Colorimetric DPD-method was used as an analytical method for the determination
260 of oxidant species. It is accepted for water analysis by standard protocols (EPA Method
261 330.5/Standard Method 4500-Cl G) in both wastewater and drinking water as well as
262 being recommended for seawater (Cha et al., 2015). This method is based on the
263 oxidation of N,N-diethyl-p-phenylendiamin (DPD) in the presence of oxidants. The
264 color intensity was measured with a Hach DR/2000 spectrophotometer. It should be

noted that, in addition to chlorine, other possible oxidants can be electro-generated and also react with DPD (Ghasemian et al., 2017). Therefore, results are represented as TRO and expressed as mg $Cl_2 \cdot L^{-1}$.

Temperature, pH, and conductivity were measured throughout the experimental samples, and variations with respect to the control (untreated samples) were not detected.

271 # 3. Results and Discussion

272 ## *3.1 Inactivation kinetic assays*

273 A battery of assays was performed in order to define inactivation kinetics of the MHB
274 after the EAOP. The dose-response curve is depicted in Figure 1 in which the decimal
275 logarithm of bacterial reduction, log (N/N_0), versus the electrical charge applied (Q) is
276 represented.

277 The experimental points exhibit a good fit (R^2=0.947; RMSE=0.392) for the Biphasic
278 inactivation model, Eq. (5) (Cerf, 1977; Geeraerd et al., 2005). Through a non-linear
279 adjustment of the experimental points, kinetic rate constants were obtained: k_1 and k_2
280 ($L \cdot Ah^{-1}$). This indicates two different phases of disinfection: primary inactivation with a
281 first-order rate constant (k_1) followed by a tailing deviation with k_2. The ***f*** parameter is
282 associated with k_1 and determines the population rate that is inactivated in the first
283 phase, i.e., ***f*** =99.96% (S.E.±0.0004) of the entire population are inactivated with k_1
284 (1082.32 $L \cdot Ah^{-1}$ (S.E.±75.62)). The remaining 0.04% is inactivated with a k_2 that is
285 near to zero (96.33 $L \cdot Ah^{-1}$ (S.E.±84.69)). Additionally, a number of calculations of
286 interest can be made by obtaining the Q necessary to reach a 4-Log reduction (0.019
287 $Ah \cdot L^{-1}$) or a 3-Log reduction (0.007 $Ah \cdot L^{-1}$), which permits an easy comparison of
288 disinfection efficacy when different kinetic models are applied (Moreno-Andrés et al.,
289 2017).

290 The same levels of inactivation were achieved for other authors; e.g., 0.01-0.02 $Ah \cdot L^{-1}$
291 are needed for total inactivation of *E. coli* (Cano et al., 2012; Lacasa et al., 2013). Other
292 authors, such as Anfruns-Estrada et al. (2017), work in different operation regimes and
293 reach at least a 4-Log reduction of diverse types of bacteria at current densities of 33.3
294 $mA \cdot cm^{-2}$ and between 20 to 90 minutes residence time. In this study, higher inactivation
295 rates were obtained with current density values of 95 $mA \cdot cm^{-2}$ but with a residence time
296 of 0.13 s in the maximum case.

297 Inactivation pathways on the EAOPs are derived from two different disinfection
298 mechanisms known as direct (at electrode surface) or indirect inactivation (Fig. A1,
299 Supp. material) (Moreira et al., 2017; Panizza and Cerisola, 2009; Särkkä et al., 2015).
300 The latter is the result of oxidants species produced either by water oxidation or by
301 substances that are dissolved in water which, in our case, is the use of seawater with
302 high concentrations of chloride ions. However, other species such as sulfate or
303 hydrogencarbonate can electro-generate additional oxidant species such as
304 peroxydisulfate or peroxodicarbonate which can be involved in disinfection processes
305 (Garcia-Segura et al., 2017).

306 The oxidation of chlorides on an anode surface leads to the formation of free chlorine
307 which is consequently hydrolyzed to form hypochlorous acid (HClO)/ hypochlorite ion
308 (ClO^-) depending on the pH of the solution. In that context, the Chlorine Active Species
309 (CAS) that were generated were represented according to the electrical charge applied
310 (Q) (Figure 2).

311 According to Figure 2, a linear trend is observed at least by the Q values that cover the
312 entire inactivation kinetics. Afterwards, a quadratic expression applies, suggesting that
313 the generation of oxidizing species will reach a limit (Fig.2-outerbox); in this aspect,
314 oxygen evolution will be the dominant process instead of the electro-generation of
315 oxidant species (Ghasemian et al., 2017; Panizza and Cerisola, 2009). According to that,
316 a direct relationship between the TRO generation and disinfection efficiency can be
317 assumed on inactivation kinetics. Nevertheless, this aspect will be discussed later in
318 Section 3.4.

319 On the other hand, the use of BDD electrodes as non-active anode material has a main
320 disadvantage which is the production of noxious ionic species (chlorate, perchlorates,
321 bromates) as a result of further oxidation of both CAS and bromide compounds
322 (Bergmann et al., 2009; Oh et al., 2010; Vacca et al., 2013). In this context, Vacca et al.

(2013) studied the behavior of both of these compounds with the EAOP on the BDD electrodes and concluded that, when Cl^- and Br^- are both present in a solution, disinfection by-products (DBPs) will depend primarily on the chloride concentration (because the generation of active chlorine is the quickest reaction). Thus, when the chloride concentration is in the amounts of seawater (in the order of 10 $g \cdot L^{-1}$), bromate production is almost completely inhibited during the electrolysis process (Vacca et al., 2013). Additionally, this speciation is significantly affected by both applied current density and flow rate, i.e., low current densities with high flow rates can reduce the formation of hazardous DBPs (Bergmann et al., 2009; Cano et al., 2012).

According to the results obtained, our current density work range was 9.72-101.38 $mA \cdot cm^{-2}$; with flow rates ranging from 200 to 1000 $L \cdot h^{-1}$. According to Bergmann et al. (2009), a small influence on perchlorate concentration is detected with flow rates >200 $L \cdot h^{-1}$. Otherwise, Cano et al. (2012) did not detect hazardous by-products (even at a trace level) with current density values of 0.13-1.3 $mA \cdot cm^{-2}$, which are quite low values compared to this study. Hence, high inactivation rates have been reached with both higher current densities as well as higher flow-rates. In terms of Q, operational values similar to those of Cano et al. (2012) were achieved. Nevertheless, one of the most significant challenges for the EAOPs is the up-scaling from lab scale to full scale; therefore, future studies are recommended to carefully investigate DBPs under real operating conditions such as high flow rates.

3.2 Recolonization after treatment

It is known that bacteria can regrow even after an apparent successful disinfection treatment (Grob and Pollet, 2016). In order to study this regrowth capability, four samples were selected in different degrees of inactivation and thus differently generated TRO (S1, S2, S3, S4); all details appear in Table 2.

348 Different strategies could be utilized after chemical disinfection. In this study, two
349 approaches were taken: i) quenching the TRO or ii) keeping it in solution. In Figure 3, it
350 can be observed how the MHB can evolve after treatment under these two strategies.

351 When the TRO was neutralized after treatment, the data reflects that bacteria can
352 recover within two days regardless of the disinfection degree that was reached (Fig.
353 3A). Significant differences between each treatment with controls were detected on S2-
354 S4 samples on Day 0 ($p<0.05$), otherwise, no statistical differences were found between
355 the treated samples compared with the control 48 hours after treatment; i.e., treated
356 samples were statistically equal to the control from Day 2 onwards. In this case,
357 recolonization occurred within two days (Fig 3A), which is what happens with other
358 types of treatments (Hess-Erga et al., 2010; Romero-Martínez et al., 2016). This
359 scenario take place with a majority of chemical options for BWTs that are used to treat
360 waters at the uptake or at the discharge, with the consequential neutralization of the
361 residual oxidant before it enters into ballast tanks. This is to avoid active substances
362 than can cause either toxic effects or corrosion in tanks (LLoyd`s Register Maritime,
363 2017).

364 On the other hand, no regrowth is observed if the TRO is kept in solution regardless of
365 the oxidant concentration (Fig. 3B). In this case, statistical differences ($p<0.05$) were
366 obtained in all of the treated samples when compared with the control from Day 1 until
367 the end of the experiment. Here, the diffusion of TRO into the cells may act as an extra-
368 factor of inactivation after treatment. The high level of cellular aggressions caused by
369 ROS may facilitate the diffusion of the disinfectant into the cell in a post-treatment
370 scenario. According to the results that were obtained, it seems to be sufficient for
371 growth inhibition.

372 Following the strategy in which the TRO is kept in a solution (in order to prevent
373 regrowth), monitoring the TRO decay is required. This ensures that the oxidant

374 concentration does not exceed the maximal discharge limit concentration; e.g., <0.5
375 $mg \cdot L^{-1}$ according to MEPC.159(55); for the discharge of treated effluents by onboard
376 wastewater treatment systems (no TRO discharge standard currently exists for ballast
377 water). In this sense, the TRO concentration was monitored over 16 days by simulating
378 a ballast tank. Results are depicted in Figure 4. In the case of samples with high
379 generated TRO (S3, S4: 10, 30 $mg \cdot L^{-1}$), complete removal was not detected within 16
380 days. Samples with 1 and 5 $mg \cdot L^{-1}$ (S1, S2) did not show detectable levels of TRO at
381 the end of the test, i.e., the TRO was completely removed on the second day (S1) while,
382 in S2, complete removal was reached on the fourth day. It is an advantage when
383 treatment is performed at the ballast water uptake whereby treated water can maintain
384 low concentrations of TRO, and total inactivation can be achieved during the ship's
385 voyage (Fig 3B and Fig 4). Additionally, at the moment of discharge, the levels of the
386 TRO will be below discharge limits. This strategy is in accordance with Echardt and
387 Kornmueller (2009).

388 ***3.3 Effects on bacterial community composition***

389 Apart from the importance of regrowth in ballast ships' tanks, the changes in the
390 bacterial community evolution is a strategic factor that must be monitored. The effects
391 caused by disinfection treatments can result in increased levels of dissolved organic
392 carbon that facilitates recolonization of surviving bacteria in receiving waters (as can be
393 seen in Section 3.2). Besides recolonization, bacterial succession dynamics are
394 important in the way that the absence of competition (low bacterial concentrations after
395 disinfection) allows easy growth for bacteria with high specific growth rates, usually
396 known as opportunists or r-strategists.

397 According to that, an approach of the bacterial community succession has been
398 performed based on the time required to form macroscopically visible colonies (Tv) as
399 is explained in Section 2.3.1. Thus, lower Tv values are associated with bacterial groups

400 exhibiting higher specific growth rates and could be related to opportunistic bacteria
401 (these are often the opportunistic pathogens). Meanwhile, higher Tv values are
402 associated with k-strategists which could be representative of an ecosystem with a
403 stable environment where high interspecific competition select slow-growing specialists
404 (Salvesen and Vadstein, 2000). This theory has direct consequences on microbial
405 ecology and ballast water implications (De Schryver and Vadstein, 2014; Hess-Erga et
406 al., 2010; Litchman, 2010).

407 Selected cases for samples taken on Days 1, 2, 4, and 8 after treatment are represented
408 in Figure 5. The percentage of bacteria that was visible on Days 1 and 2; i.e., Tv= 1 and
409 2, in respect to the total bacterial community can be observed. They are associated with
410 r-strategists with higher growth rates thus are so-called fast growers. The specific data
411 and Tv-values appear in Table A.1, Supp. Data. It is important to emphasize that the
412 data represent the case when the TRO was quenched after treatment; on the contrary, no
413 regrowth was detected (Section 3.2).

414 According to Figure 5, it can be determined that the percentage of fast growers is higher
415 in treated samples than in those that are untreated, assuming that bacterial groups with
416 higher growth rates prevail in treated samples. For example, on the first two days after
417 treatment, more than 50% of the colonies in all of the treated samples are considered r-
418 strategists. In untreated samples, a steady distribution is observed, i.e., the percentage of
419 fast growers does not exceed 35% on the first two days of incubation. After a succession
420 process (Days 4-8), those differences seem to diminish. For instance, S1 and S2
421 decrease considerably in the percentage of fast growers; otherwise, for samples S3 and
422 S4 in which a higher electrical dose (Q) was applied, the colonies of rapid growth are
423 still above 50%. That means that variations in bacterial communities after storage can
424 occur, and it seems to be related to treatment strength.

425 This transitory shift in bacterial communities can be due to several factors. These
426 factors include the greater availability of nutrients for surviving bacteria, the increase of
427 biodegradable fraction (due to the modification of organic matter after treatment) that
428 consequently rises on substrate availability, or a possible increase in resistance
429 mechanisms after oxidative damages for specific bacterial groups (Becerra-Castro et al.,
430 2016; Hess-Erga et al., 2010; Moreno-Andrés et al., 2018). Thus, despite the fact that
431 disinfection processes can be effective, a bacterial succession process can occur and,
432 consequently, different bacterial groups may be dominant. According to the data
433 obtained, it suggests that a monopolization of rapidly growing bacteria dominates the
434 system (treated samples), at least during the first days. Although it is a poorly explored
435 issue, some studies accord with this trend, in both wastewater (Becerra-Castro et al.,
436 2016) and seawater (Hess-Erga et al., 2010).

437 It is probable that the increase in opportunistic bacteria (associated with high growth
438 rates) could dominate a disturbed environment such as a post-disinfection scenario in
439 the event of ballast tanks or receiving harbor areas. This may also enhance the invasive
440 potential of aquatic invasive microbes which could lead to serious ecological, economic,
441 and health consequences (Drillet, 2016; Litchman, 2010) especially because many
442 genus of pathogens are usually detected in dominated r-selected communities (Vadstein
443 et al. in prep.). This aspect is very important in ballast water implications because all of
444 these scenarios can interfere with different ballast water management strategies. In this
445 sense, in depth studies are recommended for the specific evaluation of possible changes
446 in bacterial diversity after disinfection of ballast water.

447 ***3.4 Bacterial survival concerning to the treatment: AEOP and chlorination***

448 Finally, all of the results discussed in the previous sections are directly related to
449 inactivation mechanisms that are associated with the disinfection processes. In this
450 aspect, electrochemical processes in seawater are primarily applied for the generation of

451 CAS (Särkkä et al., 2015; Stehouwer et al., 2015; Tanaka et al., 2013). Additionally, it
452 has been demonstrated that ROS generated in electrochemical disinfection implies
453 higher disinfection efficiency (Jeong et al., 2006). With the aim of assessing a specific
454 CAS role on bacterial inactivation, it was independently evaluated by adding NaOCl.

455 In order to achieve the same concentrations of TRO as those assessed in samples S1-S4,
456 NaOCl was added in a single dosage, and the evolution of the MHB was evaluated in
457 the different microcosm experiments such as those in Section 3.2; i.e., by keeping the
458 TRO in a solution. Only slight differences of instantaneous inactivation were obtained
459 compared to the EAOP (data not shown). However, on the contrary, the evolution after
460 treatment differs significantly. Consequently, the percentage of regrowth after treatment
461 was calculated according to Eq. (6) and is represented in Figure 6.

462 According to Fig. 6, the regrowth of the MHB occurs according to different levels of
463 added chlorine; i.e., S1 (1 $mg \cdot L^{-1}$) reaches the higher values of bacterial regrowth;
464 followed by S2 and S3 (5, 10 $mg \cdot L^{-1}$), and negative values were obtained in S4. It must
465 be remembered that, according to Section 3.2, the regrowth percentage remained
466 negative for all of the samples when electro-generated TRO is kept in a solution (Fig.
467 3B). Thus, greater cellular damage occurs on the EAOP compared to NaOCl, suggesting
468 that different oxidant species besides CAS are involved in disinfection mechanisms and
469 prevent the regrowth after treatment.

470 As stated in Section 3.1, the inactivation of microorganisms in an electrolytic cell
471 follows both direct and indirect oxidation processes. Direct inactivation requires
472 bacterial adherence on the anode surface. In this regard, Ghasemian et al., (2017)
473 studied the role of bacterial adhesion on electrodes surfaces and no high inactivation
474 rates were detected; whereas it mainly depended on the type of bacteria. In addition, two
475 main indirect oxidation mechanisms are derived from either water quality (which is
476 mainly influenced by chloride concentration) or water oxidation.

The electro-oxidation of water generates different ROS (Eq. (1-4)) which can play an important role in disinfection mechanisms. In this sense, several studies considered diverse electrode materials (Jeong et al., 2009), selective hydroxyl radical probe compounds (Jing and Chaplin, 2017), or electrolyte systems (Muff et al., 2011) to determine the specific production of •OH in the EAOPs; all confirmed the high production of •OH when non-active electrodes (BDD) were used. Concretely, Jeong et al., (2009) state that •OH production by the BDD electrodes was approximately ten times higher compared to active electrodes.

Additionally, it can be assumed that chemical disinfection efficiency depends on the type of disinfectant. While CAS does not cause cell surface damage (i.e., disinfection mechanisms are based on inner cell components) (Cho et al., 2010), •OH are able to inactivate cells by mainly causing membrane or wall damages, resulting in major cell injury (Fiorentino et al., 2015). Thus, the higher bacterial damage (that avoids regrowth) detected in this study (in comparison with NaOCl), could be attributed to the electro-generation of several ROS, such as •OH, H_2O_2, and O_3 (Jeong et al., 2009, 2006).

The use of seawater as an efficient electrolyte not only implies the generation of Chlorine Active Species (CAS) but can also generate Reactive Oxygen Species (ROS), which probably are responsible for the inhibition of bacterial regrowth. Thus, future studies are recommended with the aim to define the specific role of both ROS (specially •OH) and CAS on the inactivation mechanisms. In this context, EAOPs could be optimized by ranging different key operational parameters that would allow the determination of the best ratio between ROS and CAS production, especially for marine water disinfection purposes.

3.5 Preliminary estimation of operation costs

Once disinfection efficiency was evaluated and different scenarios were exposed, the energy efficiency of the process was estimated; it was performed by considering only electricity consumption (Cano et al., 2016; Ghasemian et al., 2017). Thus, the specific energy consumption (W) can be calculated from the values of the electrical charge applied (Q) and the total applied voltage (V) (Eq. (7)) (Cano et al., 2016):

$$W\ (kWh \cdot m^{-3}) = Q \cdot V \qquad \text{Eq. (7)}$$

This was calculated for the S1-S4 samples as is shown in Table 3. According to different scenarios, a variance trough 0.009-0.264 $kWh \cdot m^{-3}$ can be seen depending on the degree of inactivation reached. For high inactivation degrees (≈4-Log red.; S3, S4), higher energy consumption is required (0.095-0.264 $kWh \cdot m^{-3}$). For low-medium degrees of inactivation, less consumption was estimated, 0.009-0.035 $kWh \cdot m^{-3}$ for samples S1 and S2, respectively. These values are slightly higher than those obtained by, e.g., Lacasa et al. (2013) or Nanayakkara et al. (2012) who required 0.009-0.088 $kWh \cdot m^{-3}$ for complete inactivation of *E. coli* in ballast water. For more resistant organisms such as *A. franciscana*, consumption increases up to 8.6 $kWh \cdot m^{-3}$ (Lacasa et al., 2013). Thus, the values obtained suggest that the MHB could be more resistant than the typical indicator established on the BWMC (such as *E. coli*).

The primary techniques used for ballast water treatment are UV radiation and electrochemical processes (LLoyd`s Register Maritime, 2017; Stehouwer et al., 2015) in which calculated values for energy consumption represent promising results when compared to those obtained when UV systems are applied. For example, Moreno-Andrés et al. (2016) estimated that 0.047 $kWh \cdot m^{-3}$ was used to reach 4-Log reductions in *E. faecalis*, which can be reduced to 0.026 $kWh \cdot m^{-3}$ if an AOP is applied (UV/H_2O_2). With the data obtained in the present study, 0.095 $kWh \cdot m^{-3}$ are required for

525 a 3.7-Log reduction of MHB. With 0.009 kWh·m^{-3} (S1), less efficiency can be obtained
526 in the first stage (2.2-Log reduction); however, by keeping the TRO in a second stage,
527 total inactivation can be achieved in three days as has been explained in Section 3.2
528 (Fig. 3A).

4. Conclusions

In this study, the suitability of an Advanced Electrochemical Oxidation Process (EAOP) with Boron Doped Diamond (BDD) electrodes for disinfection of seawater was assessed at a laboratory scale. Several aspects have been addressed by covering the entire disinfection process: inactivation kinetics and recolonization after treatment with a bacterial diversity assessment, together with an estimation of energy costs.

By assessing inactivation kinetics, a biphasic inactivation approach exhibits a good fit for Marine Heterotrophic Bacteria (MHB) by obtaining disinfection parameters such as the electrical charge applied (Q) that is needed for reaching a 4-Log reduction (0.019 $Ah \cdot L^{-1}$) or a 3-Log reduction (0.007$Ah \cdot L^{-1}$). By comparison with chlorination, it can be concluded that the use of BDD anodes induces greater cell damage when an AEOP is applied. Those cell damages are sufficient for preventing bacterial regrowth when TRO is kept in a solution.

Furthermore, bacterial community dynamics after treatment was evaluated. It was concluded that, despite disinfection processes can be effective, there is not only a capacity for regrowth after treatment but also a bacterial succession process in which different bacterial groups may be dominant. This aspect has direct implications on ballast water management. Depending on the ecosystem status of receiving waters, it may enhance the potential introduction of aquatic invasive microbes that could lead to serious ecological, economic, and health consequences.

Finally, the energy costs of the process were estimated suggesting that the EAOP is an environmentally friendly technology with low energy consumption in accordance with treatment strategy. It is an essential factor for onboard BWTs along with the capacity of production *in-situ* oxidant species, operation in mild conditions, and the smaller footprint (compact reactors). Additionally, the feasibility to work in high flow-rates, as

554 shown in this study, makes these processes a valid strategy for ballast water
555 management.

5. Acknowledgements

This work was supported by the Spanish Ministry of Economy and Competitiveness-FEDER through the R+D AVANTE Project [CTM2014-52116-R]. Javier Moreno-Andrés thanks the mobility program of the University of Cádiz: Programa de Becas UCA Internacional de Posgrado-Doctorado" Convocatoria 2016.

6. References

Aguilar, S., Rosado, D., Moreno-Andrés, J., Cartuche, L., Cruz, D., Acevedo-Merino, A., Nebot, E., 2017. Inactivation of a wild isolated Klebsiella pneumoniae by photo-chemical processes: UV-C, UV-C/H2O2 and UV-C/H2O2/Fe3+. Catal. Today In press. doi:10.1016/j.cattod.2017.10.043

Anfruns-Estrada, E., Bruguera-Casamada, C., Salvadó, H., Brillas, E., Sirés, I., Araujo, R.M., 2017. Inactivation of microbiota from urban wastewater by single and sequential electrocoagulation and electro-Fenton treatments. Water Res. 126, 450–459. doi:10.1016/j.watres.2017.09.056

Becerra-Castro, C., Macedo, G., Silva, A.M.T., Manaia, C.M., Nunes, O.C., 2016. Proteobacteria become predominant during regrowth after water disinfection. Sci. Total Environ. 573, 313–323. doi:10.1016/j.scitotenv.2016.08.054

Bergmann, M.E.H., Rollin, J., Iourtchouk, T., 2009. The occurrence of perchlorate during drinking water electrolysis using BDD anodes. Electrochim. Acta 54, 2102–2107. doi:10.1016/j.electacta.2008.09.040

Brinkmeyer, R., 2016. Diversity of bacteria in ships ballast water as revealed by next generation DNA sequencing. Mar. Pollut. Bull. 107, 277–285. doi:10.1016/j.marpolbul.2016.03.058

Cano, A., Barrera, C., Cotillas, S., Llanos, J., Cañizares, P., Rodrigo, M.A., 2016. Use of DiaCell modules for the electro-disinfection of secondary-treated wastewater with diamond anodes. Chem. Eng. J. 306, 433–440. doi:10.1016/j.cej.2016.07.090

Cano, A., Cañizares, P., Barrera-Díaz, C., Sáez, C., Rodrigo, M.A., 2012. Use of conductive-diamond electrochemical-oxidation for the disinfection of several actual treated wastewaters. Chem. Eng. J. 211–212, 463–469. doi:10.1016/j.cej.2012.09.071

587 Cerf, O., 1977. A Review Tailing of Survival Curves of Bacterial Spores. J. Appl.
588 Bacteriol. 42, 1–19. doi:10.1111/j.1365-2672.1977.tb00665.x

589 Cha, H.-G., Seo, M.-H., Lee, H.-Y., Lee, J.-H., Lee, D.-S., Shin, K., Choi, K.-H., 2015.
590 Enhancing the efficacy of electrolytic chlorination for ballast water treatment by
591 adding carbon dioxide. Mar. Pollut. Bull. 95, 315–323.
592 doi:10.1016/j.marpolbul.2015.03.025

593 Chaplin, B.P., 2014. Critical review of electrochemical advanced oxidation processes
594 for water treatment applications. Environ. Sci. Process. Impacts 16, 1182–1203.
595 doi:10.1039/C3EM00679D

596 Cho, M., Kim, J., Kim, J.Y., Yoon, J., Kim, J.-H., 2010. Mechanisms of Escherichia coli
597 inactivation by several disinfectants. Water Res. 44, 3410–8.
598 doi:10.1016/j.watres.2010.03.017

599 Cohen, A.N., Dobbs, F.C., 2015. Failure of the public health testing program for ballast
600 water treatment systems. Mar. Pollut. Bull. 91, 29–34.
601 doi:10.1016/j.marpolbul.2014.12.031

602 Comninellis, C., Chen, G., 2010. Electrochemistry for the environment, Springer. ed.
603 Springer New York LLC. doi:10.1007/978-0-387-68318-8

604 De Schryver, P., Vadstein, O., 2014. Ecological theory as a foundation to control
605 pathogenic invasion in aquaculture. ISME J. 8, 2360–8. doi:10.1038/ismej.2014.84

606 Drillet, G., 2016. Food security: Protect aquaculture from ship pathogens. Nature 539,
607 31–31. doi:10.1038/539031d

608 Echardt, J., Kornmueller, A., 2009. The advanced EctoSys electrolysis as an integral
609 part of a ballast water treatment system. Water Sci. Technol. 60, 2227–2234.
610 doi:10.2166/wst.2009.676

611 Fiorentino, A., Ferro, G., Alferez, M.C., Polo-Lopez, M.I., Fernandez-Ibañez, P., Rizzo,
612 L., 2015. Inactivation and regrowth of multidrug resistant bacteria in urban
613 wastewater after disinfection by solar-driven and chlorination processes. J.
614 Photochem. Photobiol. B Biol. 148, 43–50. doi:10.1016/j.jphotobiol.2015.03.029

615 Garcia-Segura, S., Ocon, J.D., Chong, M.N., 2017. Electrochemical Oxidation
616 Remediation of Real Wastewater Effluents − A review. Process Saf. Environ. Prot.
617 113, 48–67. doi:10.1016/j.psep.2017.09.014

618 Geeraerd, A.H., Valdramidis, V.P., Van Impe, J.F., 2005. GInaFiT, a freeware tool to
619 assess non-log-linear microbial survivor curves. Int. J. Food Microbiol. 102, 95–
620 105. doi:10.1016/j.ijfoodmicro.2004.11.038

621 GEF-UNDP-IMO, 2017. The GloBallast Story : Reflections from a Global Family.
622 London.

623 Ghasemian, S., Asadishad, B., Omanovic, S., Tufenkji, N., 2017. Electrochemical
624 disinfection of bacteria-laden water using antimony-doped tin-tungsten-oxide
625 electrodes. Water Res. 126, 299–307. doi:10.1016/j.watres.2017.09.029

626 Grob, C., Pollet, B.G., 2016. Regrowth in ship's ballast water tanks: Think again! Mar.
627 Pollut. Bull. 109, 46–48. doi:10.1016/j.marpolbul.2016.04.061

628 Hess-Erga, O.-K., Blomvågnes-Bakke, B., Vadstein, O., 2010. Recolonization by
629 heterotrophic bacteria after UV irradiation or ozonation of seawater; a simulation
630 of ballast water treatment. Water Res. 44, 5439–49.
631 doi:10.1016/j.watres.2010.06.059

632 IMO, 2004. International Convention for the Control and Management of Ships' Ballast
633 Water and Sediments. BWM/CONF/36.

634 Jeong, J., Kim, C., Yoon, J., 2009. The effect of electrode material on the generation of
635 oxidants and microbial inactivation in the electrochemical disinfection processes.

636 Water Res. 43, 895–901. doi:10.1016/j.watres.2008.11.033

637 Jeong, J., Kim, J.Y., Yoon, J., 2006. The role of reactive oxygen species in the
638 electrochemical inactivation of microorganisms. Environ. Sci. Technol. 3–4.

639 Jing, Y., Chaplin, B.P., 2017. A Mechanistic Study of the Validity of Using Hydroxyl
640 Radical Probes to Characterize Electrochemical Advanced Oxidation Processes.
641 Environ. Sci. Technol. acs.est.6b05513. doi:10.1021/acs.est.6b05513

642 Lacasa, E., Tsolaki, E., Sbokou, Z., Rodrigo, M.A., Mantzavinos, D., Diamadopoulos,
643 E., 2013. Electrochemical disinfection of simulated ballast water on conductive
644 diamond electrodes. Chem. Eng. J. 223, 516–523. doi:10.1016/j.cej.2013.03.003

645 Lindenauer, K.G., Darby, J.E.N.L., 1994. Ultraviolet disinfection of wastewater: effect
646 of dose on subsequent photoreactivation 28.

647 Litchman, E., 2010. Invisible invaders: Non-pathogenic invasive microbes in aquatic
648 and terrestrial ecosystems. Ecol. Lett. 13, 1560–1572. doi:10.1111/j.1461-
649 0248.2010.01544.x

650 LLoyd`s Register Maritime, 2017. Understanding ballast water management Guidance
651 for shipowners and operators.

652 Lymperopoulou, D.S., Dobbs, F.C., 2017. Bacterial Diversity in Ships' Ballast Water,
653 Ballast-Water Exchange, and Implications for Ship-Mediated Dispersal of
654 Microorganisms. Environ. Sci. Technol. 51, 1962–1972.
655 doi:10.1021/acs.est.6b03108

656 Moreira, F.C., Boaventura, R.A.R., Brillas, E., Vilar, V.J.P., 2017. Electrochemical
657 advanced oxidation processes: A review on their application to synthetic and real
658 wastewaters. Appl. Catal. B Environ. 202, 217–261.
659 doi:10.1016/j.apcatb.2016.08.037

660 Moreno-Andrés, J., Acevedo-Merino, A., Nebot, E., 2018. Study of marine bacteria
661 inactivation by photochemical processes : disinfection kinetics and growth
662 modeling after treatment. Environ. Sci. Pollut. Res.
663 doi:https://doi.org/10.1007/s11356-017-1185-6

664 Moreno-Andrés, J., Romero-Martínez, L., Acevedo-Merino, A., Nebot, E., 2017. UV-
665 based technologies for marine water disinfection and the application to ballast
666 water: Does salinity interfere with disinfection processes? Sci. Total Environ. 581–
667 582, 144–152. doi:10.1016/j.scitotenv.2016.12.077

668 Moreno-Andrés, J., Romero-Martínez, L., Acevedo-Merino, A., Nebot, E., 2016.
669 Determining disinfection efficiency on E. faecalis in saltwater by photolysis of
670 H2O2: Implications for ballast water treatment. Chem. Eng. J. 283, 1339–1348.
671 doi:10.1016/j.cej.2015.08.079

672 Muff, J., Bennedsen, L.R., Søgaard, E.G., 2011. Study of electrochemical bleaching of
673 p-nitrosodimethylaniline and its role as hydroxyl radical probe compound. J. Appl.
674 Electrochem. 41, 599–607. doi:10.1007/s10800-011-0268-1

675 Nanayakkara, K.G.N., Khorshed Alam, A.K.M., Zheng, Y.-M., Paul Chen, J., 2012. A
676 low-energy intensive electrochemical system for the eradication of Escherichia coli
677 from ballast water: Process development, disinfection chemistry, and kinetics
678 modeling. Mar. Pollut. Bull. 64, 1238–1245. doi:10.1016/j.marpolbul.2012.01.018

679 Oh, B.S., Oh, S.G., Hwang, Y.Y., Yu, H.W., Kang, J.W., Kim, I.S., 2010. Formation of
680 hazardous inorganic by-products during electrolysis of seawater as a disinfection
681 process for desalination. Sci. Total Environ. 408, 5958–5965.
682 doi:10.1016/j.scitotenv.2010.08.057

683 Panizza, M., Cerisola, G., 2009. Direct And Mediated Anodic Oxidation of Organic
684 Pollutants. Chem. Rev. 109, 6541–6569. doi:10.1021/cr9001319

Petrucci, E., Di Palma, L., De Luca, E., Massini, G., 2013. Biocides electrogeneration for a zero-reagent on board disinfection of ballast water. J. Appl. Electrochem. 43, 237–244. doi:10.1007/s10800-012-0507-0

Romero-Martínez, L., Moreno-Andrés, J., Acevedo-Merino, A., Nebot, E., 2016. Evaluation of ultraviolet disinfection of microalgae by growth modeling: application to ballast water treatment. J. Appl. Phycol. 28, 2831–2842. doi:10.1007/s10811-016-0838-z

Rubio, D., Nebot, E., Casanueva, J.F., Pulgarin, C., 2013. Comparative effect of simulated solar light, UV, UV/H2O2 and photo-Fenton treatment (UV-Vis/H2O2/Fe2+,3+) in the Escherichia coli inactivation in artificial seawater. Water Res. 47, 6367–79. doi:10.1016/j.watres.2013.08.006

Salvesen, I., Vadstein, O., 2000. Evaluation of plate count methods for determination of maximum specific growth rate in mixed microbial communities, and its possible application for diversity assessment. J. Appl. Microbiol. 88, 442–448. doi:10.1046/j.1365-2672.2000.00984.x

Särkkä, H., Bhatnagar, A., Sillanpää, M., 2015. Recent developments of electro-oxidation in water treatment — A review. J. Electroanal. Chem. 754, 46–56. doi:10.1016/j.jelechem.2015.06.016

Stehouwer, P.P., Buma, A., Peperzak, L., 2015. A comparison of six different ballast water treatment systems based on UV radiation, electrochlorination and chlorine dioxide. Environ. Technol. 36, 2094–2104. doi:10.1080/09593330.2015.1021858

Tanaka, T., Shimoda, M., Shionoiri, N., Hosokawa, M., Taguchi, T., Wake, H., Matsunaga, T., 2013. Electrochemical disinfection of fish pathogens in seawater without the production of a lethal concentration of chlorine using a flow reactor. J. Biosci. Bioeng. 116, 480–4. doi:10.1016/j.jbiosc.2013.04.013

710 Tsolaki, E., Diamadopoulos, E., 2010. Technologies for ballast water treatment: a
711 review. J. Chem. Technol. Biotechnol. 85, 19–32. doi:10.1002/jctb.2276

712 Tsolaki, E., Pitta, P., Diamadopoulos, E., 2010. Electrochemical disinfection of
713 simulated ballast water using Artemia salina as indicator. Chem. Eng. J. 156, 305–
714 312. doi:10.1016/j.cej.2009.10.021

715 UNCTAD, 2016. Review of Maritime Transport 2016, Review of Maritime Transport -
716 UNCTAD/RMT/2016.

717 Vacca, A., Mascia, M., Palmas, S., Mais, L., Rizzardini, S., 2013. On the formation of
718 bromate and chlorate ions during electrolysis with boron doped diamond anode for
719 seawater treatment. J. Chem. Technol. Biotechnol. 88, 2244–2251.
720 doi:10.1002/jctb.4095

721 Werschkun, B., Sommer, Y., Banerji, S., 2012. Disinfection by-products in ballast water
722 treatment: an evaluation of regulatory data. Water Res. 46, 4884–901.
723 doi:10.1016/j.watres.2012.05.034

724

725

7. List of Figures

Figure 1. Inactivation profile based on the decimal logarithm of bacterial reduction versus Electrical Charge Applied.

Figure 2. Electro-generated Total Residual Oxidant, expressed as chlorine generation, during inactivation procedures.

Figure 3. Evolution of bacteria after treatment: **A.** recolonization profile by quenching TRO and **B.** recolonization profile by keeping TRO in solution. Each data point represents mean value of 3 independent assays, with standard deviation presented as error bars.

Figure 4. Evolution of TRO after treatment. Each data point represents mean value of triplicate microcosms, with standard deviation presented as error bars.

Figure 5. Evolution of bacterial community based on percentage of fast growers; i.e., colonies that shown Tv=1 and 2. Some selected examples are shown for samples taken on Days 1, 2, 4 and 8. S1-S4 represents samples treated versus untreated ones (Unt.). Standard deviation is presented as error bars.

Figure 6. Regrowth percentage of samples inactivated with NaOCl. * S1, S2 and S3 corresponds to chlorine concentrations of 1, 5 and 10 $mg \cdot L^{-1}$, respectively (NaOCl added in a single dosage). S4 (30 $mg \cdot L^{-1}$) showed negative values for regrowth percentage.

Tables. Moreno-Andrés et al. Inactivation of marine heterotrophic bacteria in ballast water by an Electrochemical Advanced Oxidation Process

Table 1. Characterization of water matrix used for experimental.

Parameter	Mean ± S.D.	Parameter	Mean ± S.D.
pH	7.94 ± 0.05	CO_3^{2-} (mmol·L^{-1})	0.14 ± 0.01
Conductivity (mS·cm^{-1})	48.68 ± 0.88	HCO_3^- (mmol·L^{-1})	2.43 ± 0.09
Salinity (ppt)	31.77 ± 0.64	Cl^- (g·L^{-1})	16.26 ± 0.17
Temperature (ºC)*	13.45 ± 0.61	SO_4^{2-} (g·L^{-1})	1.99 ± 0.01
Turbidity (NTU)	0.24 ± 0.04	Br^- (mg·L^{-1})	43.16 ± 2.87
Dissolved Oxygen (mg O_2·L^{-1})	11.92 ± 0.38	Na^+ (g·L^{-1})	9.50 ± 0.09
Total Organic Carbon (TOC) (mg C·L^{-1})	2.13 ± 0.05	K^+ (mg·L^{-1})	366.40 ± 10.22
Dissolved Organic Carbon (DOC) (mg C·L^{-1})	2.02 ± 0.03	Ca^{2+} (mg·L^{-1})	535.73 ± 3.66
Alkalinity (mmol·L^{-1})	2.77 ± 0.07	Mg^{2+} (g·L^{-1})	1.30 ± 0.08

*Temperature at the time it was collected

Table 2. Operational parameters and inactivation values obtained for recolonization experiments (Mean value ± Standard Deviation).

Sample	Inactivation (Log Survival)	Current Density (mA·cm^{-2})	Electrical Charge Applied (Q/ Ah·L^{-1})	TRO generated as mg Cl_2·L^{-1}
S1	-0.11 ± 0.17	15.74 ± 1.60	0.002 ± 1.925E-04	1.17 ± 0.31
S2	-2.16 ± 0.28	45.83 ± 0.05	0.006 ± 1.502E-08	5.13 ± 0.12
S3	-3.60 ± 0.11	100.46 ± 1.60	0.012 ± 1.925E-04	10.50 ± 1.00
S4	-4.79 ± 0.15	100.93 ± 0.80	0.034 ± 4.078E-03	31.67 ± 4.33

Table 3. Consumption parameters and energy costs of the treatment in a theoretical possible scenario.

Sample	S1	S2	S3	S4
Energy consumption	Q: 0.002 Ah·L^{-1} V: 5.23 V W: 0.009 kWh·m^{-3}	Q: 0.006 Ah· L^{-1} V: 6.30 V W: 0.035 kWh·m^{-3}	Q: 0.012 Ah· L^{-1} V: 7.80 V W: 0.095 kWh·m^{-3}	Q: 0.034 Ah· L^{-1} V: 7.81 V W: 0.264 kWh·m^{-3}

Figure1

Click here to download high resolution image

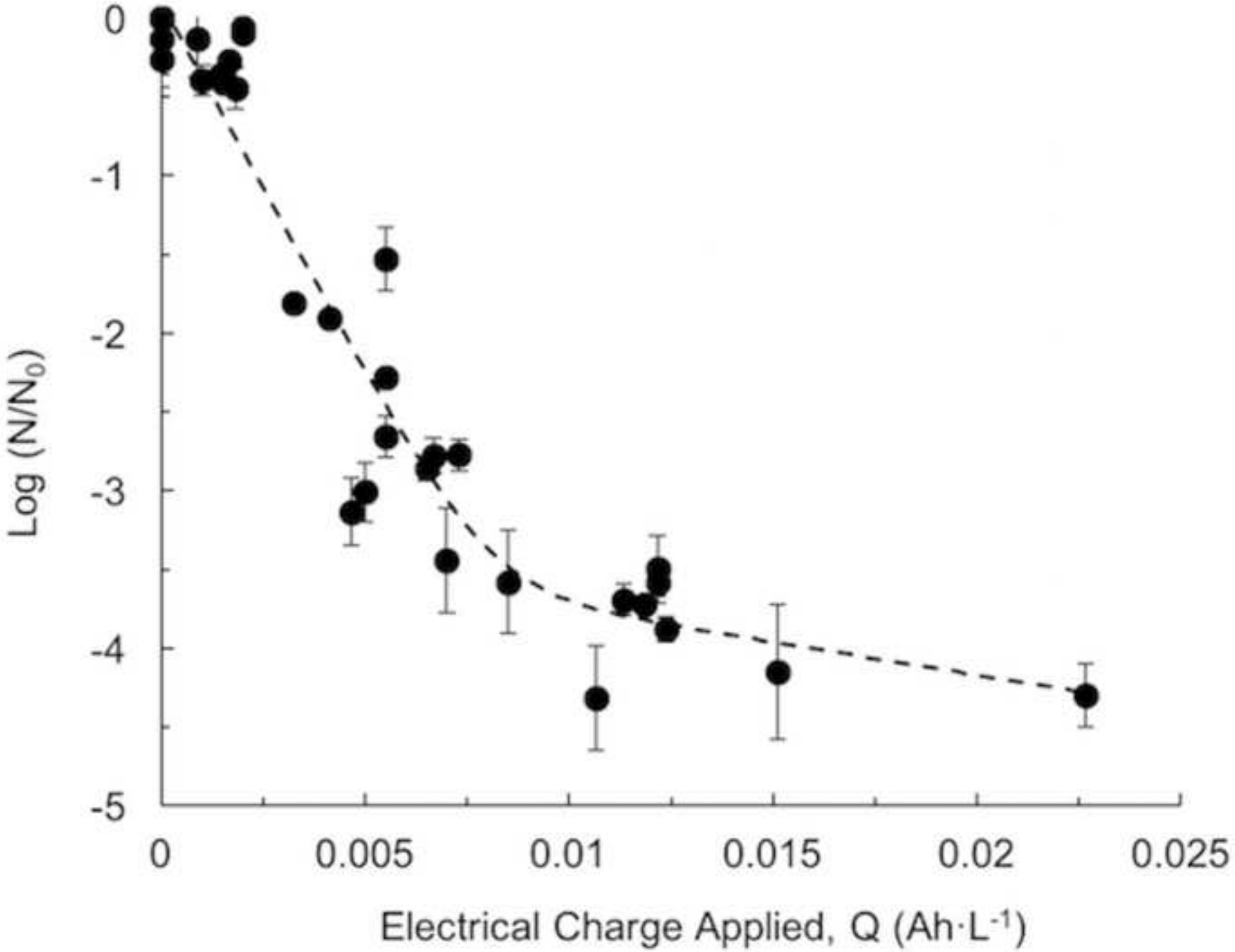

Figure2

Click here to download high resolution image

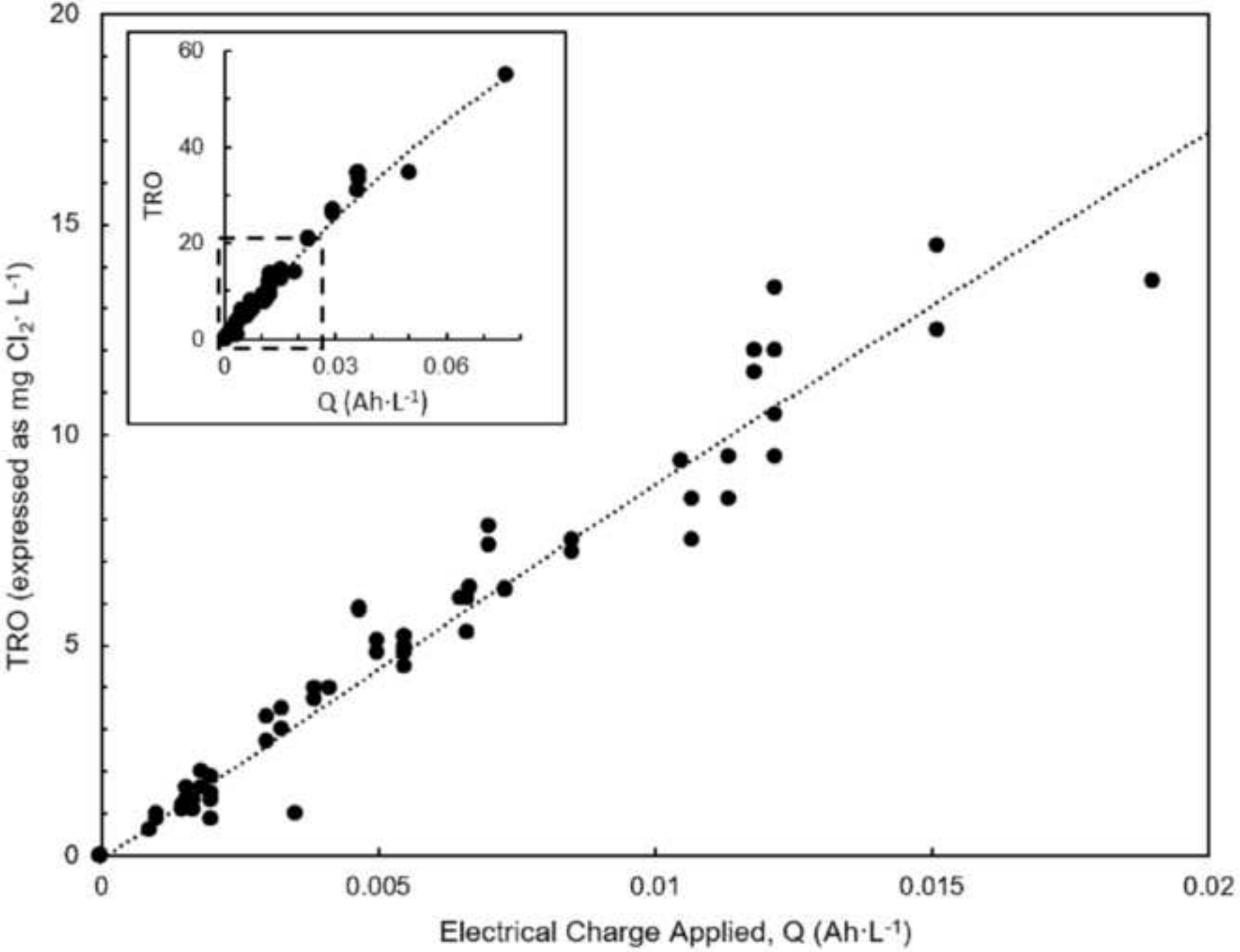

Figure3

Click here to download high resolution image

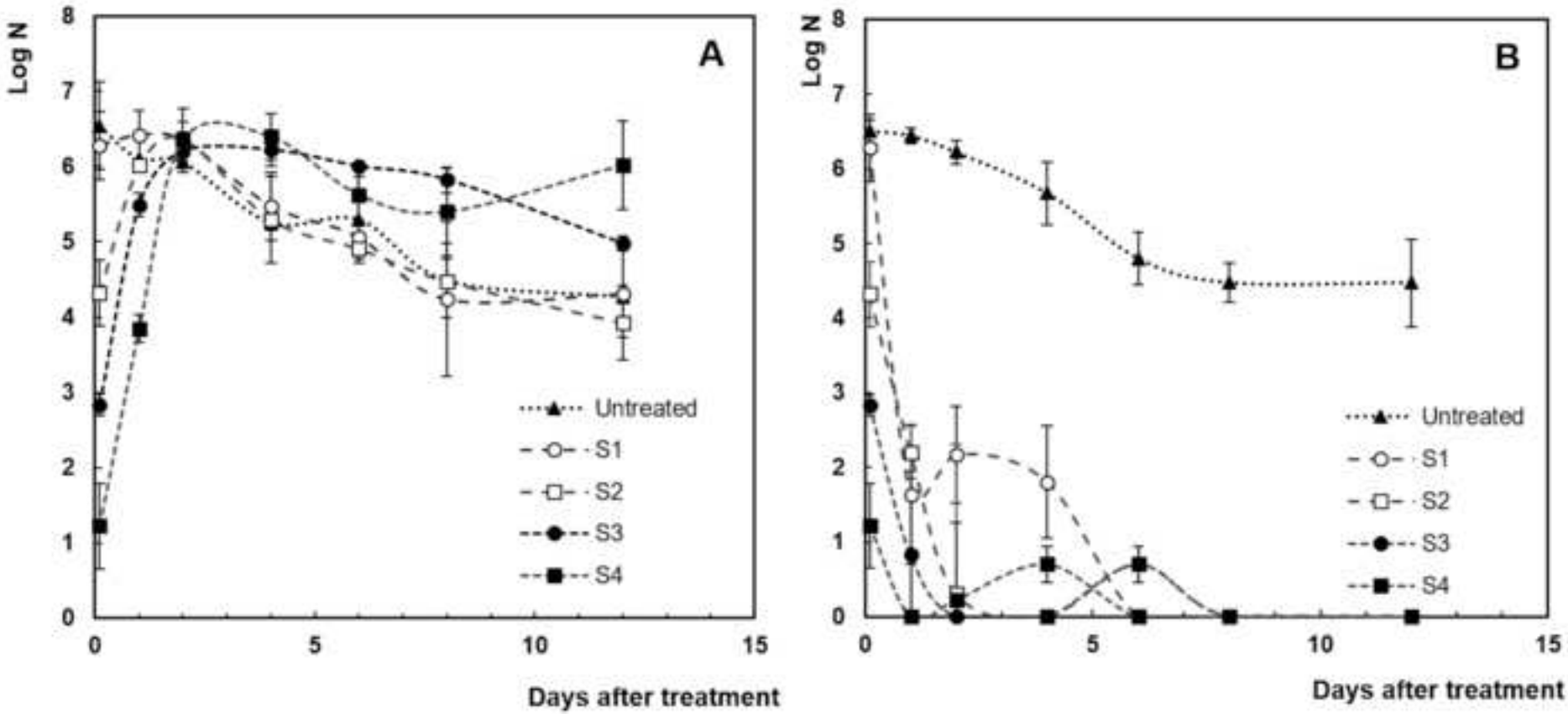

Figure4

Click here to download high resolution image

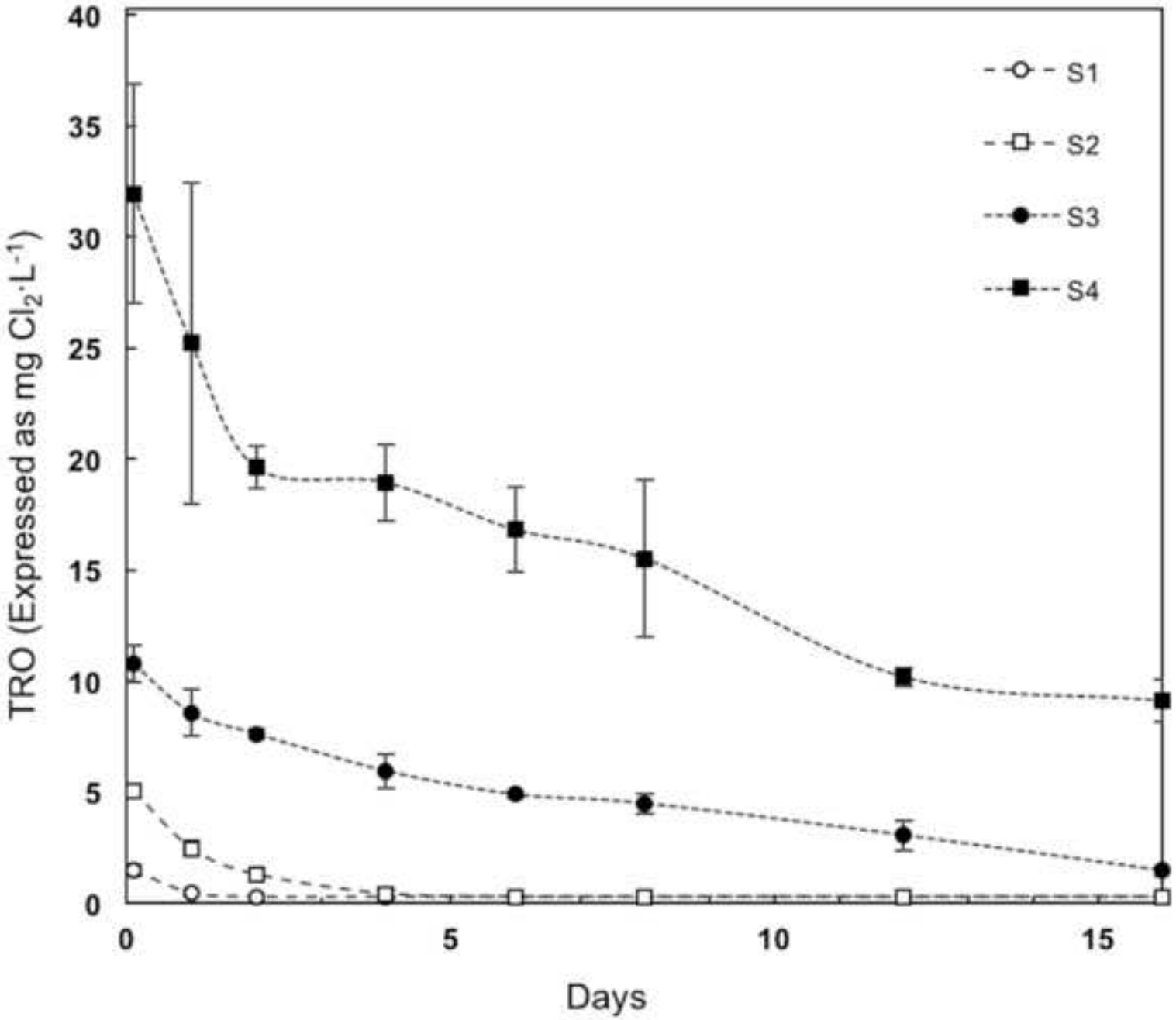

Figure5

Click here to download high resolution image

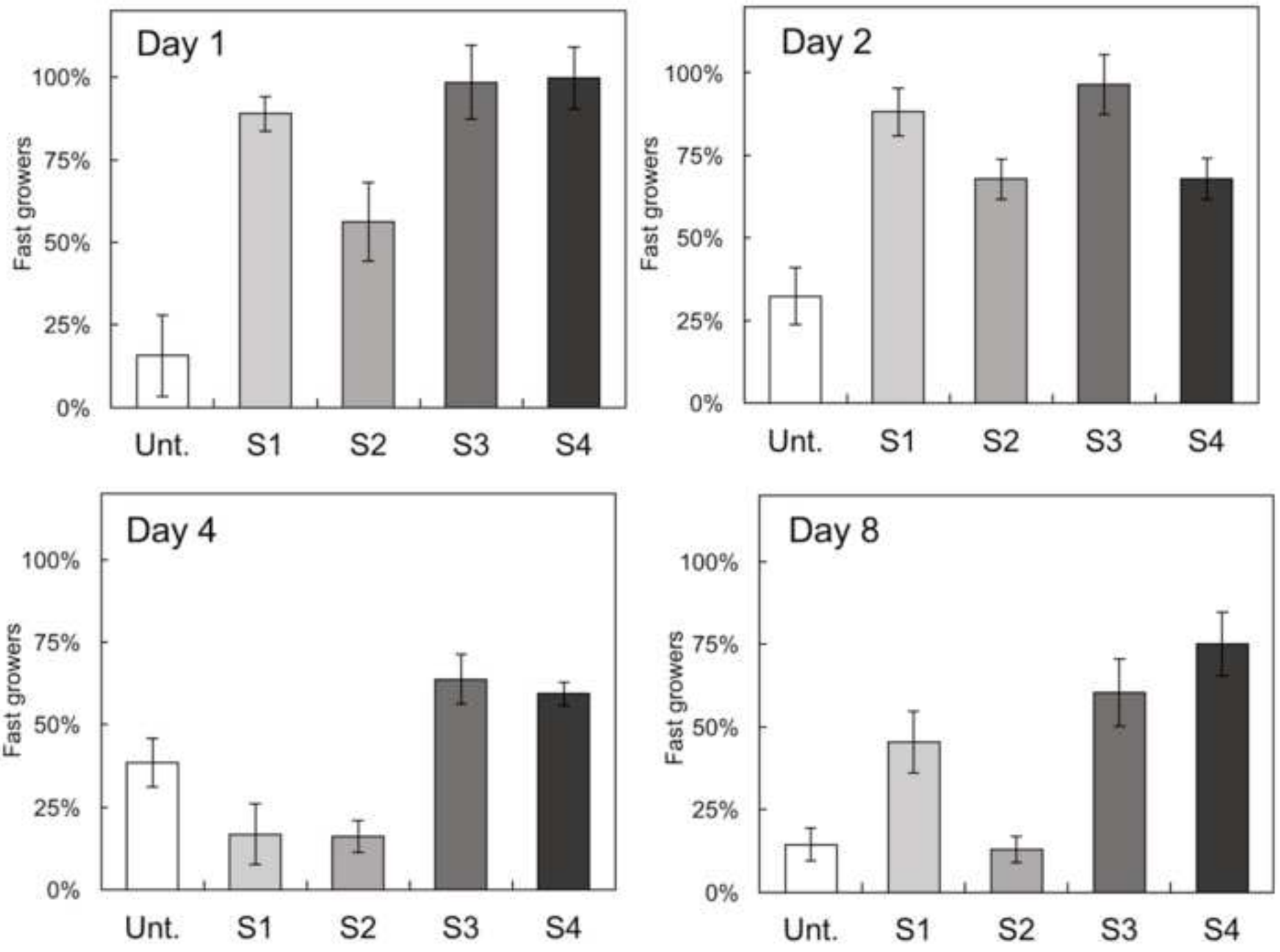

Figure6

Click here to download high resolution image

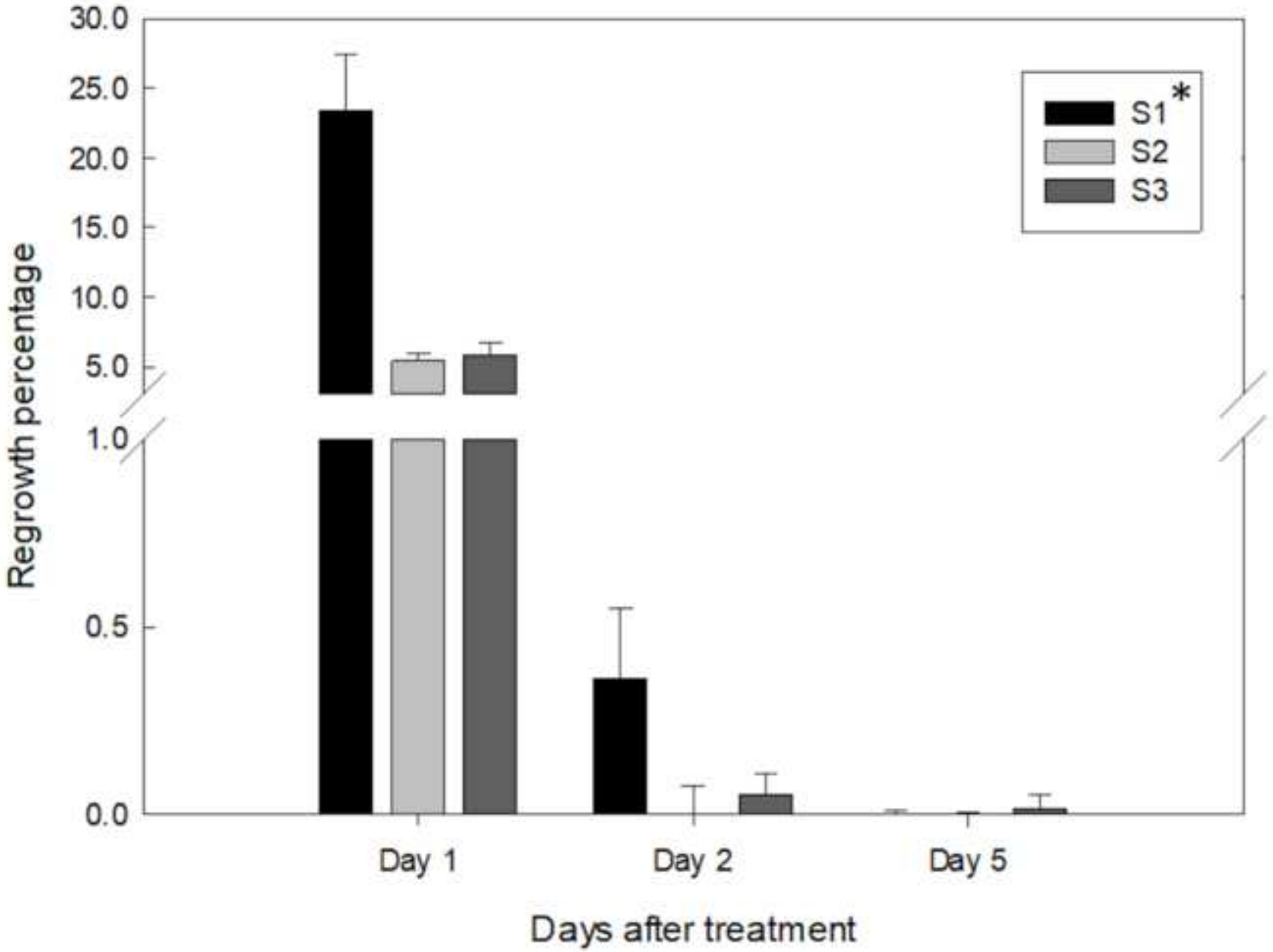

Electronic Supplementary Material (for online publication only)

Click here to download Electronic Supplementary Material (for online publication only): Supplementary material.docx